

Effects of Different Liquid Properties on the Characteristics of Impact-Generated High-Speed Liquid Jets

Anirut Matthujak* , Chaidet Kasamnimitporn, Wuttichai Sittiwong
and Kulachate Pianthong

Department of Mechanical Engineering, Faculty of Engineering
Ubon Ratchathani University (UBU)
Ubon Ratchathani, THAILAND
e-mail: Anirut.Mat@gmail.com

Keywords- high-speed liquid jet, impact acceleration method, shadowgraph, shock waves

Abstract— This paper describes the study of high-speed liquid jets injected in air from an orifice. The main focus is to study the effect of different liquid properties on the characteristics of the high-speed liquid jets injected in ambient air. The high-speed liquid jets are generated by the impact of a projectile, which known as impact acceleration method, launched in a horizontal single-stage power gun (HSSPG). The conical nozzle of 30° angle with the orifice diameter of 0.7 mm was used to generate the jets. The characteristics of high-speed jets were visualized by the high-speed digital video camera with shadowgraph optical arrangement. From the shadowgraph images, the jet formation, atomization, vaporization and shock waves were obviously observed. The maximum averaged velocity of water, alcohol, n-hexane, chloroform and glycerin jets is estimated to be 1,669.03 m/s, 1,548.59 m/s, 1,420.44 m/s, 1,204.46 m/s and 1,496.97 m/s, respectively. That effect on the maximum penetration distance of the water jet is longer than that of all jets. Surface tension and latent heat are the significant physical property for jet formation, while density, kinematics viscosity and heat capacity are not.

Introduction

High-speed liquid jet has been studied for their wide applications such as cleaning and cutting technologies, mining and tunneling [1]. The high-speed liquid jet has also gained attention in combustion and medical applications [2, 3] recently. The high-speed jets in the hypersonic range, the velocity of more than 2000 m/s, have been studied and reported [4].

For commercial applications such as cutting technologies, medical and other applications in the near future, it is however unlikely to use the hypersonic jet, since the jet velocity in the applications varies just between 800-1,400 m/s. Although, there have been some studies to clarify the characteristics of high-speed liquid jet in the velocity of less than 1,600 m/s [5, 6], such studies have focused on only fuel jets, such as diesel, gasoline and kerosene, while other liquid jets have never been reported.

In this study, the characteristics of the different liquid jets in the low supersonic range, the velocity of less than 1,600 m/s, are reported. The difference characteristics of all jets, such as jet formation, penetration distance and velocity attenuation are analyzed and described by visualization.

High-Speed Liquid Jet Generation

Liquid jets are formed when pressurized liquids confined in a container are discharged through a nozzle hole and jet speeds are determined by the value of pressures. In general, the higher pressures are, the higher the jet speed becomes. However, static pressures over GPa are hard to maintain in large volume metal vessels.

To produce high-speed jets, Bowden and Brunton [7] enhanced pressures in a liquid filled a container by a momentum transfer created with a sudden impingement of a high-speed projectile as shown in Fig. 1. Then shock waves were generated inside the container creating high pressures of

several GPa by shock compression which was maintained for a few hundred microseconds, which is even more effective than adiabatic compression. Hence to obtain higher jet speeds, impact speeds should be as high as possible technically.

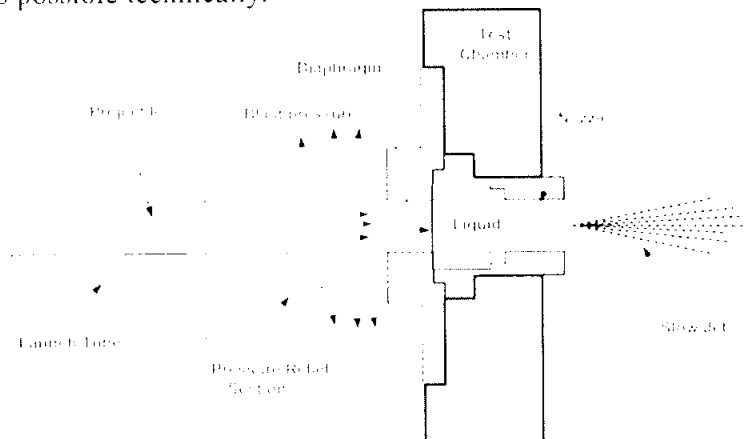


Figure 1 Experiment setup for impact acceleration method

The high velocity projectile in this technique was generated by the horizontal single stage powder gun (HSSPG) as shown in Fig. 2. The HSSPG consists of launcher, launch tube, pressure relief section and test chamber. The launch tube has a diameter of 15 mm and length of 1.5 m. The pressure relief section has a length of 38.5 cm, which is designed to diminish the blast wave in front of the projectile. The pressure relief section has 4 slots, each slot being 4 mm in width and 345 mm in length. The

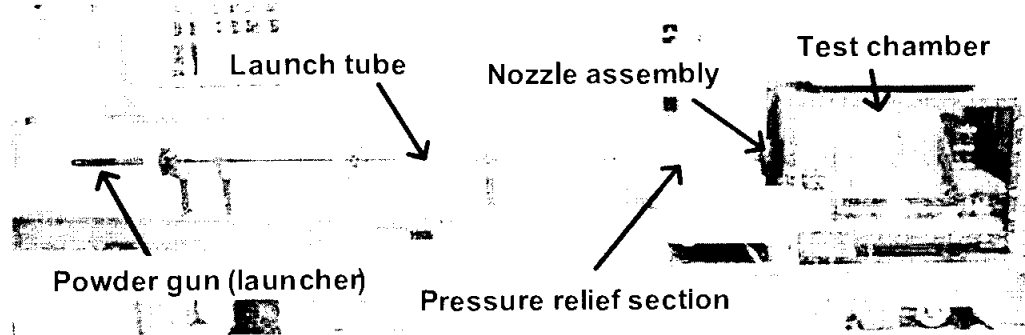


Figure 2 Horizontal Single-Stage Powder Gun (HSSPG)

test chamber is a square tank of 350 x 350 mm in width and 590 mm in length, with two polymethyl methacrylate (PMMA) windows on two sides for visualization. The projectile is made of Polymethyl Methacrylate (PMMA), is cylindrical in shape with a diameter of 15 mm and length of 8 mm (weight of 0.92 g) as shown in Fig 3a. The HSSPG can be employed to generate jet velocities of 550 to 2,290 m/s using different gunpowder weights. The nozzle that is connected to pressure relief section is made of mid-steel and its dimension is shown in Fig. 3b. In this study, gunpowder of 5 g is used which can launch the projectile at a speed of about 952 ± 32 m/s.

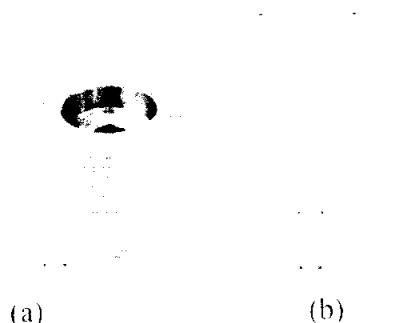


Figure 3 Nozzle geometry

Visualization Method

In this study, a high-speed digital video camera and shadowgraph optical arrangement were used to visualize the high-speed liquid jets as shown in Fig. 4. A Xenon lamp was used as a light source. The source light was collimated passing through a concave lens and a circular slit. The laboratory space was limited so that two plane mirrors of diameter 190 mm were combined. Two paraboloidal schlieren mirrors of diameter 300 mm were used for collimating source light beam passing the test section area. A Nikon 60 mm Macro lens was used to focus the object image on the high-speed digital video camera screen. The high-speed digital video camera is a Photron SA5 at frame rate of 30,000 f/s, maximum shutter speed of 1 μ s, and 5.46 seconds record time at full resolution.

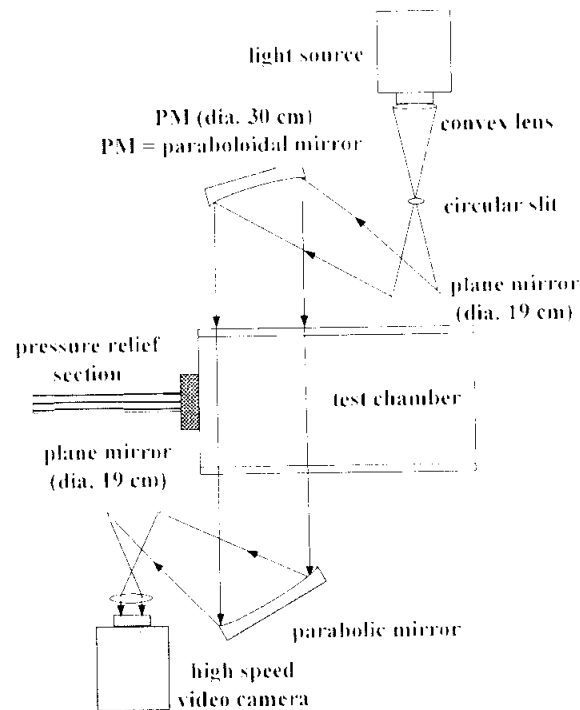


Figure 4 Shadowgraph optical setup for high-speed digital video recording

Jet Characteristics

Using a high-speed video camera, Photron SA5 could record shadowgraph images at frame rate of 30,000 f/s and shutter speed of 1 μ s. Such a sequential recording is very useful to observe the jet formation. Five liquids are investigated in this study and their properties are listed in Table. 1.

In Figure 5a, only selective 8 images are presented. Jet formations of water were discharged into atmospheric air. The water jet shows the slim width and looks more elongated to be over 213 mm at 166 μ s. Its averaged speed at 166 μ s is 1,282 m/s and Mach number (M_s) = 3.77 in room temperature air. The jet motion is supersonic so that oblique shock waves are created over its top part and also the jet's nodes. At the earlier stage, the inclination angle of the first oblique shock wave is about 15° which corresponds to the oblique shock Mach number of 3.86.

TABLE I. PROPERTIES OF LIQUIDS USED IN THE EXPERIMENT

Liquid type	Density at 25°C (kg/m ³)	Kinematics viscosity (cSt)	Surface tension at 20°C (N/m)	Heat capacity at 40°C (J/g°C)	Latent heat (kJ/kg)
Water	998	1.003 (20°C)	0.073	4.19	2,257
Alcohol	785.1	1.60 (20°C)	0.022	2.3	896
n-Hexane	654.8	0.683 (17.8°C)	0.018	2.26	365
Chloroform	1,465	0.38 (20°C)	0.027	1.05	247
Glycerin	1,259	0.648 (20.3°C)	0.063	2.43	974

The jet speed estimated from the shock inclination angle differs from that obtained from the video images. This is attributable to the fact that the relationship between the oblique shock angle and a supersonic body is valid to a supersonic solid body but in this case the jet boundary consists of distributed liquid droplets/air mixture and irregularly shaped water surface. The sound speed defined around such a jet boundary is no longer the same as that of air and slightly smaller than that in air.

In addition to this fact, the liquid jet's frontal stagnation area has a dispersed structure and a kind of ablation takes place. Not only fragmentation from bulk liquid to droplets but also vaporization on the liquid surface simultaneously takes place. As a result of it, the corresponding inclination angle of shock wave and the shock stand-off distance over the liquid jet not necessarily coincides with those over a solid body moving at the identical supersonic speed. The discrepancy also exists between the estimated jet speed from shock inclination angle and that from the video images.

Figure 5b shows alcohol jet formation. The nodes created over the alcohol jet look more bulkier than those in water jet. This trend is commonly observable in glycerin jet as shown in Fig. 5c, which is attributable to smaller values of surface tension and heat capacity. With larger surface tension the jet will not be bulged even at intermittent pressure loadings and resulting node sizes will be smaller. After elapsed time of 166 μ s, the jet speed is gradually slow which can be observed the increase of shock inclination angle. Acoustic impedances of alcohol, glycerin, n-hexane and chloroform are smaller than that of water. Hence, pressure built up in these liquids by projectile impingements at identical speeds can be less than that in water. This indicates why the water jet speed is fastest. The alcohol jet is elongated more than 213 mm at 266 μ s and is much slower than the water jet.

Figure 5c shows n-hexane jet formation. The general trend is not much different from alcohol jet up to 66 μ s. N-hexane is very volatile and hence atomization at the jets' edge promotes vaporization. The jet boundary on the images after 133 μ s looks blurred. Shock wave is attached at the jet's leading edge but after 200 μ s, it becomes a detached shock wave. The jet is quickly atomized after 200 μ s and its atomization process is quickest because its surface tension is smallest.

Figure 5d shows chloroform jet formation. Three steps of impulsive accelerations [6] are clearly observed at 100 μ s, which can be observed the change in shock angle. The general trend of the chloroform jet formation is similar to the alcohol jet formation until 200 μ s because their surface tensions are quite equal, these being 0.022 N/m and 0.027 N/m, respectively. After 200 μ s, the chloroform jet is quite similar to the n-hexane jet. The jet is attenuated as its leading edge is not elongated quickly as seen in the last three frames from 200 μ s to 333 μ s. Detached shock waves are clearly visible on the second and the third frames.

Figure 5d shows glycerin jet formation. The general trend is similar to alcohol jet even though their surface tensions are quite different, these being 0.063 N/m and 0.022 N/m, respectively. The similarity between glycerin and alcohol jets may be because their latent heats are quite equal, these being 974 kJ/kg and 896 kJ/kg, respectively.

As seen in Fig. 5, jet tips and frontal parts of nodes have dispersed structures and their boundaries are blurred. Hence, distinct shock fronts were hardly formed by these obscured fronts but compression waves were driven, which gradually coalesced into distinct oblique shock fronts. As a result of this, at the earlier stage of their formations, their edges look not necessarily a clear

boundary but appear to be a bumpy boundary. Moreover, it was found that surface tension and latent heat are the significant physical property for jet formation, while density, kinematics viscosity and heat capacity are not.

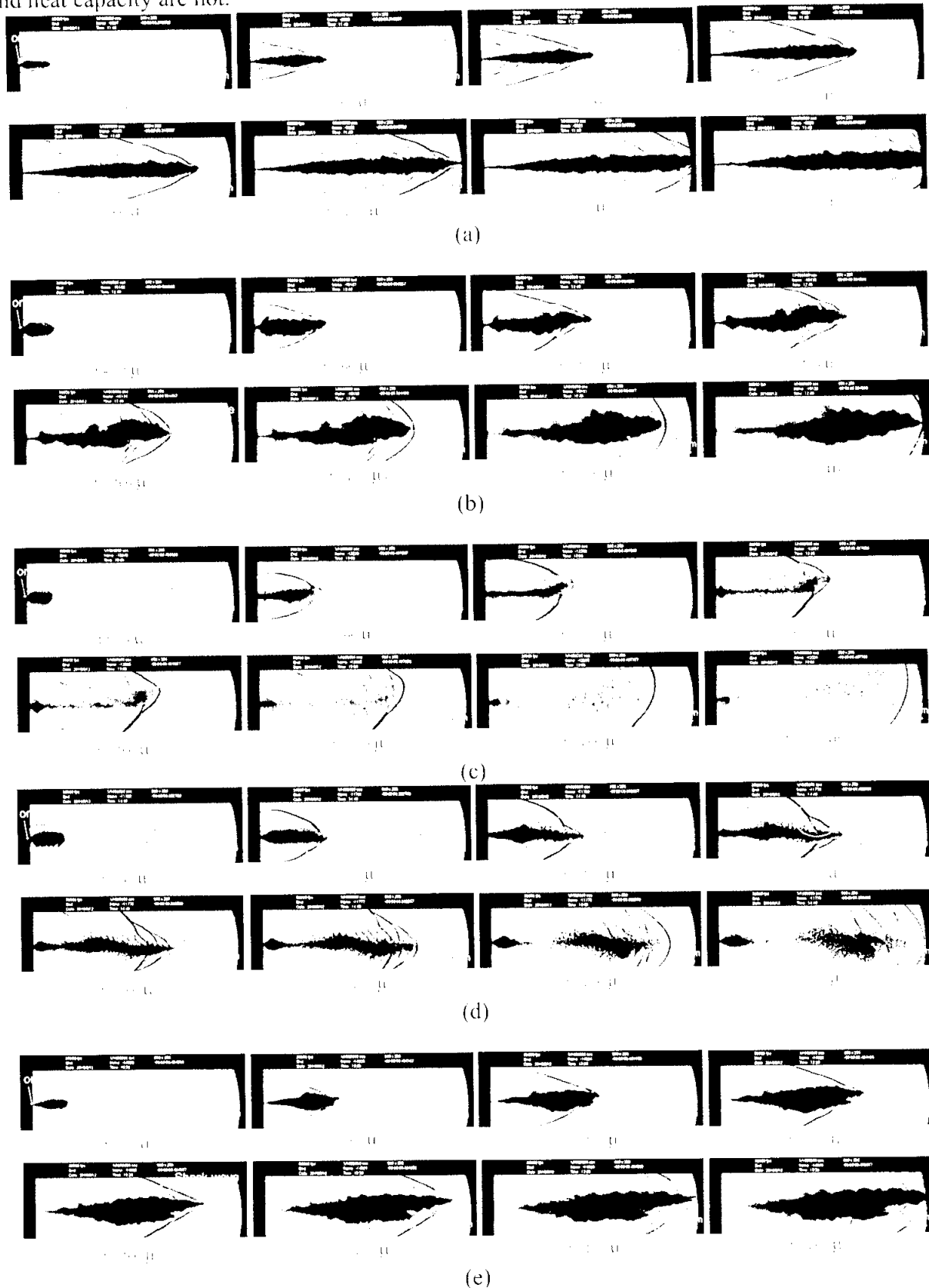


Figure 5 Jet formation (a) Water jet (b) Alcohol jet (c) n-Hexane jet (d) Chloroform jet (e) Glycerin jet

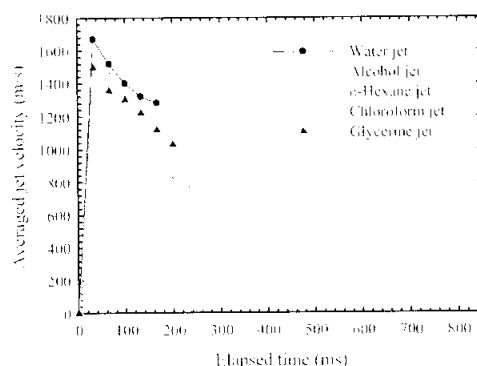


Figure 6 Effect of difference liquid jets on averaged jet velocity

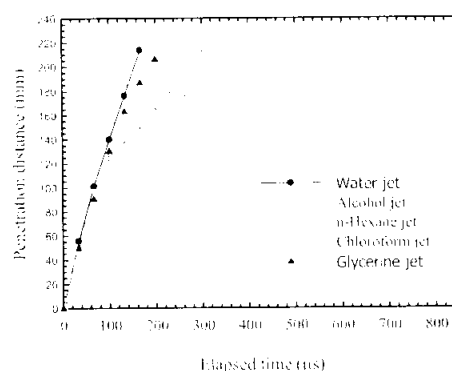


Figure 7 Effect of difference liquid jets on jet penetration distance

Fig. 6 shows the effect of different liquid jets on the averaged jet velocity. During the maximum velocity point and the emerging time of 33 μ s, the velocity of all liquid jets gradually drops as obviously seen in the figure. The maximum averaged velocity of water jet is fastest, it being estimated to be 1,669.03 m/s. The next one is alcohol, glycerin, chloroform, and n-hexane jets, respectively, these being estimated to be 1,548.59 m/s, 1,420.44 m/s, 1,204.46 m/s and 1,496.97 m/s, respectively. That effect on the penetration distance of water jet is longest at the same elapsed time as shown in Fig. 7. The second one is alcohol, glycerin and chloroform jets, respectively. The shortest penetration distance is n-hexane jet. It can be concluded that the higher surface tension is, the faster the maximum averaged jet is and the longer the jet penetration distance is even though the alcohol jet does not play this role. It may be due to the latent heat of the alcohol jet which effects on the atomization and vaporization process. However, the different characteristics of alcohol jet from all liquid jets still needs more experiments to clearly describe or confirm the occurrence.

Concluding Remarks

This study describes the characteristics of high-speed water, alcohol, n-hexane, chloroform and glycerin jets injected in ambient air. Using a high-speed digital video camera with shadowgraph optical arrangement, the dynamic behaviors of all jets and their shock waves were clearly observed. Formation of water, alcohol and glycerin jets are similar, while formation of n-hexane and chloroform jet are similar which atomization was obviously observed in the later stage. Special behaviors being three steps of impulsive accelerations and change in shock angle were clearly observed in chloroform jet. The maximum averaged velocity of water, alcohol, n-hexane, chloroform and glycerin jets is estimated to be 1,669.03 m/s, 1,548.59 m/s, 1,420.44 m/s, 1,204.46 m/s and 1,496.97 m/s, respectively. That effect on the maximum penetration distance of the water jet is longer than that of all jets. Surface tension and latent heat are the significant physical property for jet formation, while density, kinematics viscosity and heat capacity are not.

Acknowledgment

The authors are grateful to Thailand Research Fund (TRF, contact No.MRG5180046), Department of Mechanical Engineering, Faculty of Engineering, Ubon Ratchathani University (UBU), National Research Council of Thailand (NRCT) and Thailand Toray Science Foundation (TTSF) for financial support.

References

- [1] M.C. Rochester and J.H. Brunton, "High speed impact of liquid jets on solid," 1st International Symposium on Jet Cutting Technology, paper A1, Coventry, UK, 1972.
- [2] F.S. Billig, "Research on supersonic combustion," *Journal of Propulsion and Power*, vol. 9 (4), 1993, pp. 499-514.
- [3] T. Ohki, A. Nakagawa, T. Tominaga and K. Takayama, "Experimental application of Pulsed Ho: YAG laser-induced liquid jet as a novel device for rigid neuroendoscope," *Laser Surg Med*, vol. 34, 2004, pp. 227.
- [4] K. Pianthong, K. Takayama, B.E. Milton, and M. Behnia, "Multiple pulsed hypersonic liquid diesel fuel jets driven by projectile impact," *Shock Waves Journal*, vol. 14, 2005, pp. 73-82.
- [5] A. Matthujak, K. Pianthong, M. Sun, K. Takayama and T. Ikohagi, "Effects of different fuels on the characteristics of supersonic liquid jets," *The 25th International Symposium on Shock Waves*, Bangalore, India, pp 1111-1117, July 2005.
- [6] Matthujak, S.H.R. Hosseini, K. Takayama and P. Voinovich, "High-speed liquid jet formation by impact acceleration method," *Shock wave*, vol. 16 (6), 2007, pp. 405-419.
- [7] F.P. Bowden and J.H. Brunton, "Damage to solids by liquid impact at supersonics speeds," *Nature*, vol. 181, 1958, pp. 873-875.

1
2
3
4
5
6
7
8
9
10
11
12
13
14
15
16
17
18
19
20
21
22
23
24
25
26
27
28
29
30
31
32
33
34
35
36
37
38
39
40
41
42
43
44
45
46
47
48
49
50
51
52
53
54
55
56
57
58
59
60
61
62
63
64
65
66
67
68
69
70
71
72
73
74
75
76
77
78
79
80
81
82
83
84
85
86
87
88
89
90
91
92
93
94
95
96
97
98
99
100
101
102
103
104
105
106
107
108
109
110
111
112
113
114
115
116
117
118
119
120
121
122
123
124
125
126
127
128
129
130
131
132
133
134
135
136
137
138
139
140
141
142
143
144
145
146
147
148
149
150
151
152
153
154
155
156
157
158
159
160
161
162
163
164
165
166
167
168
169
170
171
172
173
174
175
176
177
178
179
180
181
182
183
184
185
186
187
188
189
190
191
192
193
194
195
196
197
198
199
200
201
202
203
204
205
206
207
208
209
210
211
212
213
214
215
216
217
218
219
220
221
222
223
224
225
226
227
228
229
230
231
232
233
234
235
236
237
238
239
240
241
242
243
244
245
246
247
248
249
250
251
252
253
254
255
256
257
258
259
260
261
262
263
264
265
266
267
268
269
270
271
272
273
274
275
276
277
278
279
280
281
282
283
284
285
286
287
288
289
290
291
292
293
294
295
296
297
298
299
300
301
302
303
304
305
306
307
308
309
310
311
312
313
314
315
316
317
318
319
320
321
322
323
324
325
326
327
328
329
330
331
332
333
334
335
336
337
338
339
340
341
342
343
344
345
346
347
348
349
350
351
352
353
354
355
356
357
358
359
360
361
362
363
364
365
366
367
368
369
370
371
372
373
374
375
376
377
378
379
380
381
382
383
384
385
386
387
388
389
390
391
392
393
394
395
396
397
398
399
400
401
402
403
404
405
406
407
408
409
410
411
412
413
414
415
416
417
418
419
420
421
422
423
424
425
426
427
428
429
430
431
432
433
434
435
436
437
438
439
440
441
442
443
444
445
446
447
448
449
450
451
452
453
454
455
456
457
458
459
460
461
462
463
464
465
466
467
468
469
470
471
472
473
474
475
476
477
478
479
480
481
482
483
484
485
486
487
488
489
490
491
492
493
494
495
496
497
498
499
500
501
502
503
504
505
506
507
508
509
510
511
512
513
514
515
516
517
518
519
520
521
522
523
524
525
526
527
528
529
530
531
532
533
534
535
536
537
538
539
540
541
542
543
544
545
546
547
548
549
550
551
552
553
554
555
556
557
558
559
560
561
562
563
564
565
566
567
568
569
570
571
572
573
574
575
576
577
578
579
580
581
582
583
584
585
586
587
588
589
590
591
592
593
594
595
596
597
598
599
600
601
602
603
604
605
606
607
608
609
610
611
612
613
614
615
616
617
618
619
620
621
622
623
624
625
626
627
628
629
630
631
632
633
634
635
636
637
638
639
640
641
642
643
644
645
646
647
648
649
650
651
652
653
654
655
656
657
658
659
660
661
662
663
664
665
666
667
668
669
670
671
672
673
674
675
676
677
678
679
680
681
682
683
684
685
686
687
688
689
690
691
692
693
694
695
696
697
698
699
700
701
702
703
704
705
706
707
708
709
710
711
712
713
714
715
716
717
718
719
720
721
722
723
724
725
726
727
728
729
730
731
732
733
734
735
736
737
738
739
740
741
742
743
744
745
746
747
748
749
750
751
752
753
754
755
756
757
758
759
760
761
762
763
764
765
766
767
768
769
770
771
772
773
774
775
776
777
778
779
780
781
782
783
784
785
786
787
788
789
790
791
792
793
794
795
796
797
798
799
800
801
802
803
804
805
806
807
808
809
810
811
812
813
814
815
816
817
818
819
820
821
822
823
824
825
826
827
828
829
830
831
832
833
834
835
836
837
838
839
840
841
842
843
844
845
846
847
848
849
850
851
852
853
854
855
856
857
858
859
860
861
862
863
864
865
866
867
868
869
870
871
872
873
874
875
876
877
878
879
880
881
882
883
884
885
886
887
888
889
890
891
892
893
894
895
896
897
898
899
900
901
902
903
904
905
906
907
908
909
910
911
912
913
914
915
916
917
918
919
920
921
922
923
924
925
926
927
928
929
930
931
932
933
934
935
936
937
938
939
940
941
942
943
944
945
946
947
948
949
950
951
952
953
954
955
956
957
958
959
960
961
962
963
964
965
966
967
968
969
970
971
972
973
974
975
976
977
978
979
980
981
982
983
984
985
986
987
988
989
990
991
992
993
994
995
996
997
998
999
1000



Applied Mechanics and Materials
Vols. 1-1000

[Home](#)
[Journal Rankings](#)
[Journal Search](#)
[Country Rankings](#)
[Country Search](#)
[Compare](#)
[Map Generator](#)
[Help](#)
[About Us](#)

Show this information in
your own website

[Journal Search](#)
 Search query

☐ Exact phrase

 in Journal Title
Applied Mechanics and Materials
Country: Switzerland

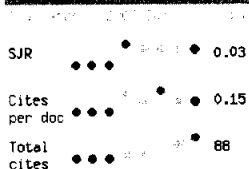
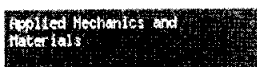
Subject Area: Engineering

Subject Category: Engineering (miscellaneous)

Publisher: Scitec Publications Ltd., **Publication type:** Book Series, **ISSN:** 16609336

Coverage: 2005-2010

H Index: 6

[Charts](#) [Data](#)

☐ Display journal title

Just copy the code below and
paste within your html page:

```
<a href="http://www.scimagojr.com/journalsearch.php?q=4700151914...">
```



How to cite this website?

SJR is developed by:

SCIMAGO

Powered by
SCOPUS

The SJR indicator measures the scientific influence of the average article in a journal, it expresses how central to the global scientific discussion an average article of the journal is. Cites per Doc. (2y) measures the scientific impact of an average article published in the journal, it is computed using the same formula that journal impact factor™ (Thomson Reuters).

Citation vs. Self-Citation

Evolution of the total number of citations and journal's self-citations received by a journal's

1

2

3

4

5

6

7

8

9

10

11

12

13

14

15

16

17

18

19

20

21

22

23

24

25

26

27

28

29

30

31

32

33

34

35

36

37

38

39

40

41

42

43

44

45

46

47

48

49

50

51

52

53

54

55

56

57

58

59

60

61

62

63

64

65

66

67

68

69

70